Rate Memory of Structural Relaxation in Glasses and Its Detection by Multidimensional NMR

A. Heuer,[1] M. Wilhelm,[1] H. Zimmermann,[2] and H. W. Spiess[1]

[1]*Max-Planck-Institut für Polymerforschung, Ackermannweg 10, D-55128 Mainz, Germany*

[2]*Max-Planck-Institut für Medizinische Forschung, Jahnstrasse 29, D-69120 Heidelberg, Germany*

(Received 5 June 1995)

A new aspect of the nature of the relaxation rate distribution of α relaxation in glasses is analyzed for the example of a polymer: How long does a polymer segment remember its relaxation rate? For a two-state system we describe the rate memory in terms of a single dimensionless parameter. Applying the theory to multidimensional NMR exchange experiments, the rate memory of a polymer slightly above its glass transition temperature is determined. The rate memory is near its theoretical minimum, indicating strong coupling of the individual relaxation modes.

PACS numbers: 64.70.Pf, 76.60.–k

The nature of the glass transition is of great interest for the understanding of amorphous systems. One of its central features is the divergence of the time scale of structural relaxation (α relaxation) near the glass transition temperature T_g [1]. The time dependence of the correlation function associated with α relaxation can be described by a stretched exponential function, the inverse Laplace transformation which corresponds to a distribution $G_0(1/\tau)$ of the relaxation rates. Structural relaxation in glasses is a cooperative, nonlocal phenomenon [2–6]. With multidimensional NMR experiments [7] on polymers, it has been shown that α relaxation is related to conformational transitions and reorientations of polymer segments [8]. The rotational dynamics of chains can be described by a combination of small angle fluctuations and large angle jumps [9]. Since multidimensional NMR techniques monitor the rotational motion on time scales between 1 ms and 10 s, information about the α process can be obtained close to T_g [7].

Because of the cooperativity of the α relaxation, the rotational dynamics of a given polymer chain segment is governed by a time-dependent potential. Therefore its relaxation rate, which we define as the probability of a rotational jump per unit of time, may vary with time. Although experimental as well as theoretical elucidation of this problem is essential for understanding the microscopic nature of the α relaxation and hence of the glass transition, only little progress has been achieved until now [9–13]. This reflects the fact that most experimental methods are incapable of obtaining this information. In this Letter we show that due to experimental *and* theoretical progress the rate memory of structural relaxation, which is a measure of the *correlation* between the *current* relaxation rate of a given polymer segment and its *initial* rate at the beginning of the experiment, can now be determined.

A possible way to obtain this correlation is sketched in Fig. 1. In the first step, one applies a filter to the sample in thermal equilibrium with a relaxation rate distribution $G_0(1/\tau)$ [Fig. 1(a)]. The filter selects all polymer segments which have not yet relaxed from the beginning of the experiment until t_{m1}. At t_{m1}, only a narrower distribution $G(1/\tau)$ for slow segments with relaxation rates $1/\tau < 1/t_{m1}$ [Fig. 1(b)] remains. After waiting for a variable time t_{m2}, one applies the same filter in order to check how the distribution of relaxation rates of the slow subensemble changed during t_{m2}. For large t_{m2} this distribution will transform to the equilibrium distribution $G_0(1/\tau)$. This is accompanied by a reduction of the number of segments which can pass the filter [Fig. 1(c)]. Deviations from $G_0(1/\tau)$ at intermediate t_{m2} are a measure of the rate memory.

First, we show that it is possible to realize the scheme of Fig. 1 by means of multidimensional solid-state NMR [7,11]. Experimental data are presented for polyvinylacetate (PVAc) slightly above T_g. Second, we develop a theoretical description, which quantifies the rate memory of structural relaxation in terms of a dimensionless parameter Q. Third, we show that the predictions of the theory

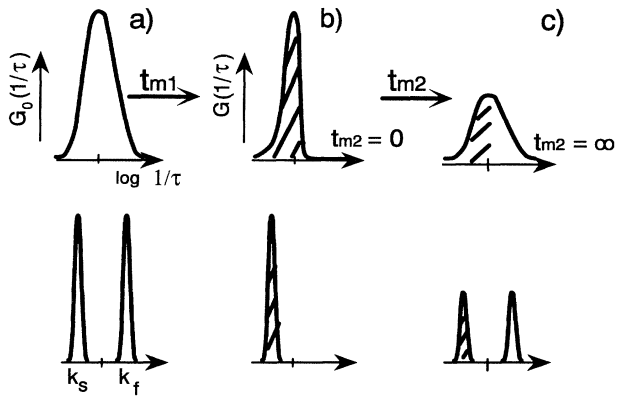

FIG. 1. Schematic presentation of the idea behind the NMR experiment introduced in the text. In the first step, a slow subensemble with a narrower rate distribution $G(1/\tau)$ than the rate distribution $G_0(1/\tau)$ of the entire sample is selected. Subsequently, the evolution to $G_0(1/\tau)$ during t_{m2} is monitored. The corresponding scheme for a two-state system is shown in the lower half.

are consistent with the experimental data. Hence we can extract the value of Q for the rate memory of structural relaxation in PVAc.

A suitable correlation function of rotational motion, and hence $G_0(1/\tau)$, can be obtained by correlating the orientation of the system at two different times which is recorded, e.g., by two-dimensional (2D) exchange NMR [7]. It detects reorientations that occur during a mixing time t_m by measuring the orientation-dependent NMR frequencies before and after t_m [14]. For the pulse sequence shown in Fig. 2(a) one obtains an echo given by $F_2(t_m) \equiv \langle \cos \omega_1 t_p \cos \omega_2 t_p \rangle$, where the frequencies ω_1 and ω_2 are the NMR frequencies of the individual molecules before and after the mixing time, and the brackets are the average over the whole system. Molecules for which the orientation does not change appreciably during t_m (i.e., $\omega_1 \approx \omega_2$) determine the echo height. If t_p is chosen sufficiently large, the contributions of the segments which perform a rotational jump average out. The time dependence of the echo height can often be well described by a stretched exponential, hence $F_2(t) = \exp[-(t/\tau_0)^\beta]$ with $\beta < 1$.

Our goal is to correlate the relaxation rate at two different times. This requires that the system is monitored at four subsequent times. The pulse sequence of such a reduced 4D NMR experiment is shown in Fig. 2(b). The odd-numbered pulses rotate the magnetization into the x-y plane perpendicular to the applied static magnetic field and let it precess freely in that plane, while the even-numbered pulses rotate the developed magnetization back. After the first mixing time t_{m1}, a slow subensemble with $\omega_1 \approx \omega_2$ generates an echo. By a pulse applied at the time of the echo maximum this selected magnetization is stored along the static magnetic field during t_{m2}. Finally, a 2D experiment with mixing time t_{m3} is performed on this subensemble. Using an appropriate phase cycling scheme, one can achieve that the final echo is proportional to $\langle \cos(\omega_1 - \omega_2) t_p \cos \omega_3 t_p \cos \omega_4 t_p \rangle$. Readers who are not familiar with multidimensional NMR techniques may take this four-point correlation function as the starting point for the theoretical analysis of the experiment.

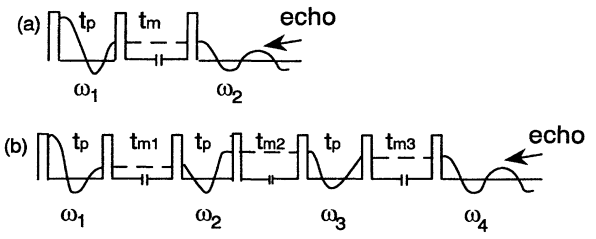

FIG. 2. Pulse sequences for exchange NMR experiments: (a) 2D experiment with one mixing time and (b) reduced 4D experiment with three mixing times (see also Ref. [11]). 90° pulses are indicated.

This four-point correlation function, normalized to its value at $t_{m2} = 0$, will be denoted as $F_4(t_{m2})$. The dominant contributions to the final echo stem from molecules which did not perform significant reorientations during t_{m1} and t_{m3}. It is easy to check that segments with $\omega_1 = \omega_2 = \omega_3 = \omega_4$, and $\omega_1 = \omega_2 \neq \omega_3 = \omega_4$ contribute in the same way to $F_4(t_{m2})$ so that the final echo is invariant whether or not rotational dynamics takes place during t_{m2} (see also Ref. [7], p. 289). Therefore the scheme of Fig. 1 is fully realized by the reduced 4D experiment. We note in passing that this statement does not hold for the correlation function resulting from a single setting of the phases of the rf pulses in Fig. 2(b) $\langle \cos \omega_1 t_p \cos \omega_2 t_p \cos \omega_3 t_p \cos \omega_4 t_p \rangle$. The underlying reason is that $\langle \cos^4 \varphi_{1234} \rangle$ is different from $\langle \cos^2 \varphi_{12} \rangle \langle \cos^2 \varphi_{34} \rangle$, where the brackets denote the average from 0 to 2π.

Our sample of PVAc [11] was selectively labeled with ^{13}C (40% enriched) at the carbonyl site, which is a convenient sensor of structural relaxation. In contrast to a similar experiment reported earlier, it is then no longer necessary to separate the contributions of the different carbon atoms so that it was possible to perform the time saving echo experiment described above, rather than recording the corresponding reduced 4D NMR spectra [11].

The experiments were performed at $T = 320$ K $= T_g + 20$ K with $t_p = 300$ μs and $t_{m1} = t_{m3} = 16$ ms ($\equiv t_{m0}$). At that temperature, T_1 is of the order of seconds and thus much longer than all time delays in the 4D pulse sequence. Thus the experimental data are void of any relaxation effects. In the first experiment we determined $F_2(t)$ [Fig. 3(a)]. The experimental data

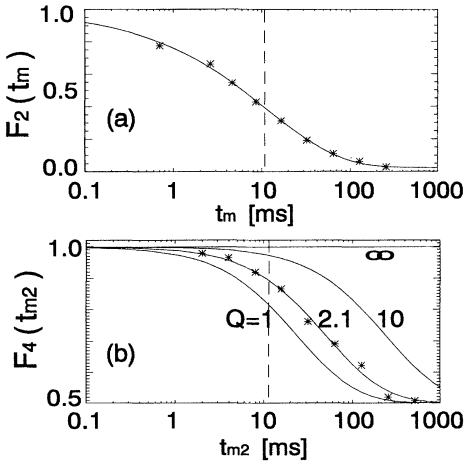

FIG. 3. The results of the NMR exchange experiments at $T = 320$ K: (a) $F_2(t_m)$ and (b) $F_4(t_{m2})$. The fit in (a) yields $\tau_0 = 11$ ms (indicated by the dashed line) and $\beta = 0.52$. The solids lines in (b) represent the theoretical curves for four values of the rate memory parameter Q. Values for τ_0 and β are taken from (a).

can be described by a stretched exponential with $\tau_0 = 11$ ms and $\beta = 0.52$. In order to obtain information about the rate memory we determined $F_4(t_{m2})$ for a number of mixing times t_{m2} [see Fig. 3(b)]. As discussed above, this experiment determines how the relaxation rate distribution of the slow subensemble approaches $G_0(1/\tau)$. First we note that our results on PVAc are consistent with those of Ref. [11] where it was found that for $t_{m2} \approx \tau_0$ the slow subensemble is still slow, whereas for $t_{m2} \approx 100\tau_0$ it behaves more like the average ensemble. The new information of our experiment concerns the whole crossover between both limiting cases. This, for the first time, allows a quantitative analysis of the rate memory of structural relaxation.

For a qualitative understanding of the information contained in $F_4(t_{m2})$, we first discuss a simple two-state model. In it, at any given moment, a polymer segment belongs either to the fast or to the slow state. A segment in the one state may switch with exchange rate Γ to the other state, and vice versa. This exchange rate mimics the fluctuations of the environment that the segment experiences. If the population of both states is the same, $F_2(t_m)$ is given by a biexponential function

$$F_2(t_m) = \frac{1}{2}[\exp(-\kappa_s t_m) + \exp(-\kappa_f t_m)], \quad (1)$$

where κ_s and κ_f are the effective slow and fast rates, respectively [cf. Fig. 4(a)]. It should be mentioned that for $\Gamma \neq 0$, κ_s and κ_f differ from the intrinsic rates k_s and k_f which would appear in $F_2(t_m)$ if no exchange were present. One has approximately $\kappa_{s,f} \approx k_{s,f} + \Gamma$. For a closer discussion see Refs. [15,16]. Let κ_s and $1/t_{m0}$ be much smaller than κ_f. Restrictions on Γ are imposed only indirectly, since for $\Gamma \to \infty$ one always has $\kappa_f \approx \kappa_s$, in contradiction to the above assumption. After waiting for a time $t_{m1} = t_{m0}$, all fast components have reoriented and only slow components remain in their original orientation. As outlined above, the magnetization of that subsensemble is stored during t_{m2} along the static magnetic field. Let $z_s(t_{m2})$ and $z_f(t_{m2})$ be the time-dependent populations of the slow and the fast state of the subensemble, respectively, during the second mixing time [Fig. 4(a)]. Under the conditions mentioned above, the initial conditions are $z_s(0) = \exp(-\kappa_s t_{m1})/2$ and $z_f(0) = 0$. Then the exchange process between the two states yields a gradual equilibration of the two populations via $z_s(t_{m2}) = z_s(0)[1 + \exp(-2\Gamma t_{m2})]/2$ and $z_f(t_{m2}) = z_s(0)[1 - \exp(-2\Gamma t_{m2})]/2$ [cf. Fig. 4(b)]. The factor of 2 can be rationalized by solving the rate equations which govern the exchange between the slow and the fast state. This population is the initial condition for the final echo experiment of the full reduced 4D experiment. The final echo height is given by $f(t_{m2}, t_{m3}) \equiv z_s(t_{m2})\exp(-\kappa_s t_{m3}) + z_f(t_{m2})\exp(-\kappa_f t_{m3})$. The dependence of the echo height on t_{m2} and t_{m3} is displayed in Fig. 4(b). In our experiment the final echo is proportional to $f(t_{m2}, t_{m3} = t_{m0})$. Under the conditions mentioned above and taking into account the normalization by $f(0, t_{m0})$, one readily obtains

$$F_4(t_{m2}) = [1 + \exp(-2\Gamma t_{m2})]/2. \quad (2)$$

Note that $F_4(t_{m2})$ depends exclusively on the exchange rate Γ, whereas it is independent of the relaxation rates κ_s and κ_f. The transition between both limiting values (here, 1 and 1/2) monitors the rate memory in real time.

As a simple quantitative measure of the rate memory, we consider the dimensionless ratio $Q = \kappa_s/\Gamma$ which counts the number of relaxation processes until a slow segment changes its rate. It can easily be determined by comparing the decay of $F_2(t_m)$ and $F_4(t_{m2})$. Low Q values indicate strong coupling between the different relaxation modes responsible for the dynamic process under study and hence a fast decay of $F_4(t_{m2})$ to the final plateau value. Because of the relation $Q = \kappa_s/\Gamma \approx (k_s + \Gamma)/\Gamma \geq 1$, the value of Q is always larger than 1. Hence one has an absolute scale for the rate memory parameter.

The concept of rate memory can be generalized to continuous rate distributions for which the parameter Q

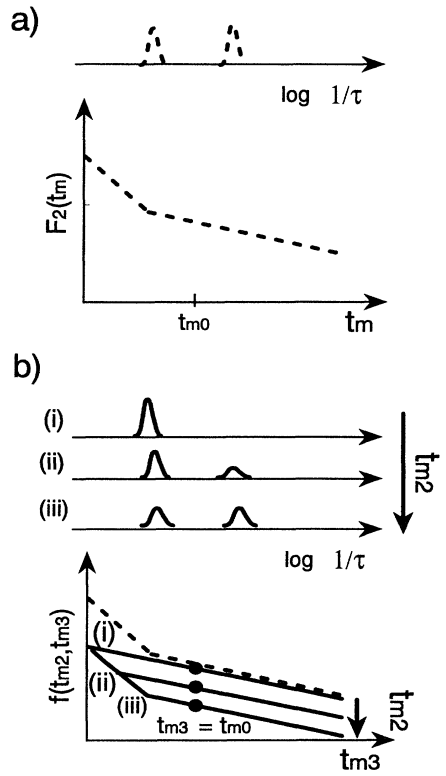

FIG. 4. Schematic analysis of the two-state model. (a) Time dependence of $F_2(t_m)$ in a semilogarithmic plot. (b) t_{m2} dependence of the selected slow subensemble [(i) $t_{m2} = 0$, (ii) intermediate t_{m2}, (iii) $t_{m2} \to \infty$] and of $f(t_{m2}, t_{m3})$. The experimental data $F_4(t_{m2})$, given as $f(t_{m2}, t_{m3} = t_{m0})/f(t_{m2} = 0, t_{m3} = t_{m0})$, are indicated by solid dots. $F_2(t_{m3})$ from (a) is indicated by the dashed line.

can be introduced in a very general way [16]. Thus, even for general functions $F_2(t_m)$, we can readily generate theoretical decay curves of $F_4(t_{m2})$ in dependence of the parameter Q. For the two-state case presented above, the relation $Q = \kappa_s/\Gamma$ follows from general theory. One can show that, in contrast to the simple limit presented above, the lower limit of Q can be as low as $1/2$.

If $F_2(t_m)$ is fitted by a biexponential function and $F_4(t_{m2})$ is determined according to Eq. (2) or if instead $F_4(t_{m2})$ is calculated according to the general formalism, identical results are arrived at, taking into account the experimental uncertainties. The experimental data in Fig. 3(b) agree very well with $Q = 2.1$. Hence for PVAc, after about two relaxation processes, no information about the dynamical history is left, and the rate memory is only twice as large as its theoretical minimum. This indicates a very strong cooperativity of α relaxation.

A related aspect concerns possible *spatial* dynamical heterogeneities around the glass transition, i.e., extended clusters of slow segments. A recent dielectric relaxation experiment on quinoxaline in a glass-forming solvent gave the first indications that the existence of heterogeneities involving more than 300 molecules can be excluded [17]. In contrast, simulations of the spin-facilitated Ising model [18] indicate the existence of spatial heterogeneities. Our results cannot settle this question, but it seems plausible that large spatial heterogeneities are only consistent with a large rate memory. However, a relation between the rate memory and spatial heterogeneities has yet to be established.

In summary, we have introduced the rate memory of glasses as a new experimental observable. For the example of PVAc we have shown that the rate memory, quantified by the parameter Q, can be determined by applying multidimensional exchange NMR. The low value of Q indicates that a strong coupling between different relaxation modes is responsible for α relaxation. It has to be noted that multidimensional NMR is restricted to probing dynamics much slower than the processes considered in the mode coupling theory [19]. By virtue of multidimensional EPR spectroscopy, [20] as well as by computer simulations, this time gap can be reduced. Work along this line in progress.

We would like to thank Professor H. Sillescu for very helpful comments. Furthermore, we acknowledge stimulating discussions with Professor F. Fujara, Professor K. Schmidt-Rohr, S. C. Kuebler, and Dr. J. Leisen. This work was supported by the DFG (SFB 262).

[1] J. Jäckle, Rep. Prog. Phys. **49**, 171 (1986).
[2] G. Adam and J. H. Gibbs, J. Chem. Phys. **28**, 373 (1965).
[3] K. L. Ngai, A. K. Rajagopal, and S. Teitler, J. Chem. Phys. **88**, 6088 (1988).
[4] E. J. Donth, J. Non-Cryst. Solids **53**, 325 (1982).
[5] C. K. Hall and E. Helfand, J. Chem. Phys. **77**, 3275 (1982).
[6] P. Ray and K. Binder, Europhys. Lett. **27**, 53 (1994).
[7] K. Schmidt-Rohr and H. W. Spiess, *Multidimensional Solid-State NMR and Polymers* (Academic, London, 1994).
[8] K. Zemke, B. F. Chmelka, K. Schmidt-Rohr, and H. W. Spiess, Macromolecules **24**, 6874 (1991).
[9] J. Leisen, K. Schmidt-Rohr, and H. W. Spiess, J. Non-Cryst. Solids **172–174**, 737 (1994).
[10] R. Richert, Macromolecules **21**, 923 (1988).
[11] K. Schmidt-Rohr and H. W. Spiess, Phys. Rev. Lett. **66**, 3020 (1991).
[12] J. Leisen, K. Schmidt-Rohr, and H. W. Spiess, Physica (Amsterdam) **201A**, 79 (1993).
[13] J. I. Kaplan and A. N. Garroway, J. Magn. Reson. **49**, 464 (1982).
[14] C. Schmidt, S. Wefing, B. Blümich, and H. W. Spiess, Chem. Phys. Lett. **130**, 84 (1986).
[15] H. Sillscu (to be published).
[16] A. Heuer (to be published).
[17] R. Richert, Chem. Phys. Lett. **216**, 223 (1993).
[18] S. Butler and P. Harrowell, J. Chem. Phys. **95**, 4454 (1991).
[19] W. Götze and L. Sjögren, Rep. Prog. Phys. **55**, 241 (1992).
[20] G. G. Maresch, M. Weber, A. A. Dubinskii, and H. W. Spiess, Chem. Phys. Lett. **193**, 134 (1992).